Available online at www.sciencedirect.com

SciVerse ScienceDirect

Ceramics International 39 (2013) 29–37

CERAMICS INTERNATIONAL

www.elsevier.com/locate/ceramint

Effect of zirconia tape porosity on fluorapatite surface film formation by dip coating

María P. Albano*, Liliana B. Garrido

Centro de Tecnología de Recursos Minerales y Cerámica (CETMIC), Camino Centenario 49, M. B. Gonnet (B1897ZCA), Provincia de Buenos Aires, Argentina

Received 17 April 2012; accepted 29 May 2012
Available online 5 June 2012

Abstract

Thin fluorapatite (FA) layers on porous 3 mol% yttria-partially stabilized zirconia (Y-PSZ) substrates have been fabricated by dipping porous zirconia tapes into aqueous 27.4 vol% fluorapatite slurries. Two porous Y-PSZ tapes with different volume fraction of porosity were developed using an acrylic latex binder: tapes with 31.4 vol% porosity were prepared using 16.6 vol% starch as fugitive additive and those with 12.7 vol% porosity were fabricated without starch. The influence of the porous structure of the tape surfaces, top and bottom, on the casting rate and consequently on the layer thickness formed on each surface was studied. Layers formed on the top and bottom surfaces of the tapes with 12.7 and 31.4 vol% porosity were compared. The formation of a thin layer on the surface of the tape was governed by both liquid entrainment and slip casting mechanisms. The data for the FA layer formation were in good agreement with the slip casting model for immersion times > 0. The casting rate at the top surface of both tapes was greater than that at the bottom surface. This difference was attributed to a greater porosity of the top surface with respect to that of the bottom one and was more pronounced for the tapes prepared with starch. Layers formed on the top surface were found to be about 55 and 32% thicker than those formed on the bottom surface for the tapes fabricated with and without starch, respectively. For the tapes prepared with starch, the greater porosity and number of smaller pores in the matrix of the top surface increased the casting rate and produced the thickest dip coated layers

Keywords: Porous ZrO_2 tapes; Fluorapatite layer; Dip coating

1. Introduction

Calcium orthophosphates such as fluorapatite ($Ca_{10}(PO_4)_6F_2$) are widely used as bone substitute materials due to their chemical similarity to the mineral component of mammalian bones and teeth [1,2]. Fluorapatite is non-toxic, biocompatible, not recognized as foreign material in the body and, most importantly, exhibits bioactive behavior and integrates into living tissue by the same processes active in remodeling healthy bone. These characteristics lead to an intimate physicochemical bond between the implants and bone, termed osteointegration [3]. Even so, the major limitations to use fluorapatite as load-bearing biomaterials is its mechanical properties, it is brittle with a poor fatigue resistance [4]. The poor mechanical behavior is even more evident for highly porous ceramics and scaffolds [5]; that is why, in biomedical applications fluorapatite is used primarily as fillers and coatings. Bioinert ceramic such as porous ZrO_2 can be coated with FA to achieve a high mechanical strength as well as a suitable biocompatibility of the system [6,7].

The currently used coating methods, such as plasma spraying, sol–gel synthesis, physical vapor deposition and dip coating, have their own advantages as well as shortcomings. The coating layer by the plasma-spraying technique is thick (~50–200 μm) and relatively dense; however, phase instability and non-uniformity are some of its weaknesses [8,9]. The films synthesized by sol–gel and physical vapor deposition methods are relatively uniform and the fabrication method is simple; however, the layer is too thin (~1 μm) to be applied for long-term usage [10,11].

*Corresponding autor. Fax: +54 0221 471 0075.
E-mail address: palbano@cetmic.unlp.edu.ar (M.P. Albano).

0272-8842/$36.00
http://dx.doi.org/10.1016/j.ceramint.2012.05.089

Coating layers dense and uniform with thickness of 5–20 μm retaining high chemical and thermal stability can be produced by dip coating. When a dry porous substrate is dipped into a ceramic suspension and subsequently withdrawn from it, a wet dense cake of well-defined thickness can be formed on the substrate surface. After being dried and sintered, a ceramic layer is achieved.

We have previously studied the tape casting process to produce porous zirconia substrates using starch and an acrylic latex emulsion as fugitive additive and binder, respectively [12–15]. Besides, the processing of stable concentrated aqueous FA suspensions with the addition of ammonium polyacrylate (NH_4PA) and Poly(vinyl)alcohol (PVA) as dispersant and binder, respectively, was investigated [16,17]. In this work, porous Y-PSZ tapes with two different volume fraction of porosity (12.7 and 31.4 vol%) were produced by tape casting and characterized with specific attention directed to the microstructure of the top and bottom surfaces of the sintered tapes. Then, sections of these tapes were dip coated into a concentrated aqueous FA slurry to produce thin FA layers.

Two mechanisms govern the formation of a layer on a porous body during dip coating. The first mechanism is known as liquid entrainment, and occurs as the plate-like specimen is withdrawn from the slurry faster than the liquid can drain from its surface, leaving a thin slurry film [18]. The second mechanism is slip casting, the capillary suction caused by the porous substrate drives ceramic particles to concentrate at the substrate-suspension boundary, and a wet layer is formed [19]. The withdrawal velocity and the suspension properties (volume fraction of solids, viscosity) have influence on the liquid entrainment mechanism; and the microstructure of the substrate (porosity and pore diameter) together with the suspension properties have influence on the slip casting mechanism. In this work, the withdrawal velocity and suspension properties were fixed, therefore the influence of the porous structure of the tape surfaces, top and bottom, on the casting rate and consequently on the layer thickness formed on each surface was studied. Layers formed on the top and bottom surfaces of the tapes with 12.7 and 31.4 vol% porosity were compared. These results would be essential for fabrication of uniform FA layers on porous zirconia tapes using the dip coating procedure.

2. Experimental procedure

2.1. Materials

2.1.1. Y-PSZ tapes

A commercial 3 mol% yttria-partially stabilized zirconia doped with 0.3 wt% Al_2O_3 (Saint-Gobain ZirPro, China) was used to produce the cast tapes. The mean particle diameter and the specific surface area were 0.15 μm and 12.25 m^2/g, respectively. Potato starch commercially available in Argentina was used as pore former agent. The starch granules exhibit a small degree of anisotropy with a median equivalent diameter of about 50 μm.

A commercial ammonium polyacrylate (NH_4PA) solution (Duramax D 3500, Rohm & Haas, Philadelphia PA) was used as a dispersant. The binder was an acrylic latex emulsion (Duramax B1000, Rohm & Haas, Philadelphia PA) with solids loading of 55 wt%,an average particle size of 0.37 μm, and a glass transition temperature of −26 °C.

2.1.2. Fa slurries

The $Ca_3(PO_4)_2$ (Fluka, Germany) and CaF_2 (Sigma–Aldrich, Ireland) powders were mixed in stoichiometric ratio and calcined 3 h at 1000 °C. Then, the powder was milled in an attrition mill using 1.6 mm zirconia balls with 0.047 wt% NH_4PA during 48 h. The milled powder was washed with distilled water and dried at 100 °C. This powder subsequently referred as FA was used to prepare the suspensions for dip coating. NH_4PA and a 9 wt% PVA solutions were used as deflocculant and binder, respectively. The degree of hydrolysis of PVA was 87–89% and the average molecular weight was in the range of 57000–66000 g/mol.

2.2. Slip preparation

2.2.1. Y-PSZ tapes

Concentrated aqueous Y-PSZ suspensions with a solid loading of 77 wt% were prepared by deagglomeration of the powder in distilled water with 0.3 wt% NH_4PA (dry weight base of powder) using an ultrasonic bath. For the tapes prepared with starch, 13 wt% of starch (dry weight base of Y-PSZ powder) was added to the stabilized Y-PSZ slips followed by ultrasonic treatment. Subsequent to this, 25 wt% latex (dry weight basis with respect to (Y-PSZ + starch) powders) was added to the slurry, followed by additional stirring. The pH of the suspensions was adjusted to 9.0 with ammonia (25 wt%).

2.2.2. FA slurries

27.4 vol% aqueous FA slips with 0.6 wt% NH_4PA and 5 wt% PVA were prepared by suspending particles in deionized water via 20 min of ultrasound; the pH was manually adjusted to be maintained at 9.

2.3. Tape-casting, burnout and sintering

The Y-PSZ slips were cast manually on a Mylar film using an extensor. The gap between the extensor and the film was adjusted to 0.4 mm. The cast tapes were subsequently dried in air at room temperature up to constant weight; afterwards, they were stripped from the film and sectioned into rectangular pieces of 2.75 cm × 1.65 cm. The burn out of organic additives was achieved by slow heating (1 °C/min) up to 1000 °C. Then, the pre-calcined tapes were sintered at 1500 °C for 2 h, with a heating rate of 5 °C/min.

2.4. Characterization

2.4.1. Y-PSZ tapes

The tapes were weighed and measured geometrically to determine the green density. The bulk sintered density was calculated from the dimensions and weight of the sintered pieces. In order to calculate the relative green and sintered densities, density values of 6.05 and 1.45 g/cm^3 were used for Y-PSZ and starch, respectively.

The open porosity and the pore size distribution of the sintered tapes were determined using mercury porosimetry (Porosimeter 2000 Carlo Erba, Italy). The microstructure of sintered samples were observed on both the top side of the tape (exposed to air during casting/drying), and the bottom side (exposed to the carrier surface during casting/drying) using a scanning electron microscopy (SEM JEOL, JSM-6360). The fractured surfaces of the tapes were also examined by SEM.

2.4.2. FA slurries

The viscosity of 27.4 vol% slips with 0.6 wt% NH_4PA and 5 wt% PVA was measured. Steady state flow curves of FA slips were performed by measuring the steady shear stress value as a function of shear rate in the range from 0.5 to 542 s^{-1}using a concentric cylinder viscometer (Haake VT550, Germany) at 25 °C. A coaxial cylinder system with two gaps (sensor system NV Haake) was used. As soon as stationary conditions were reached at each shear rate, the shear rate increased in steps up to the maximum value and then decreased.

2.5. Dip coating

The sintered tapes were vertically dipped into the FA suspension; after immersion during different times they were withdrawn from the suspension. All specimens were immersed and withdrawn at a constant rate of 8 mm/s. The dip-coated samples were allowed to dry at room temperature in the vertical orientation, further dried in air at 60 °C, heated for 30 min at 600 °C for binder burn out and sintered at 1200 °C for 1 h.

2.6. Characterization of dip-coated tapes

Dipped tapes were diamond polished and examined by SEM; the layer thickness on the top and bottom surfaces was measured. The weight gain of the dip-coated tapes was also determined.

3. Results and discussion

3.1. Characterization of green and sintered tapes

Table 1 shows the composition and properties of green and sintered Y-PSZ tapes prepared with and without starch. We can define the following expressions:

$$v_s = \text{volume of starch/bulk 0 green volume}(v_T) \quad (1)$$

V_S=volume of starch/volume of starch+volume of Y-PSZ+volume of latex+volume of pores

$$F_{vs} = \text{volume of starch/volume of solids} = \text{volume of starch/volume of starch} + \text{volum of Y}-\text{PSZ} + \text{volume of latex} \quad (2)$$

$$F_{vz} = \text{volum of Y}-\text{PSZ/volume of solids} \quad (3)$$

$$F_{vL} = \text{volume of latex/volume of solids} \quad (4)$$

V_S indicates the volume of starch relative to the volume of the green tape; whereas, F_{VS} is the volume of starch with respect to the volume of solids.

The relative green density of the tapes with volume fraction of starch (V_S) of 0 and 16.6% was nearly the same; this suggested that the addition of starch to the Y-PSZ tape did not introduce additional porosity. The volume fraction of starch in the green tape (V_S) was slightly lower than the volume fraction of added starch (F_{VS}), due to the presence of some residual porosity in the green body.

The bulk Y-PSZ packing density in the matrix can be expressed by

$$d_{ysz} = \text{volume of Y}-\text{PSZ}/(v_T - \text{volume of starch}) \quad (5)$$

This parameter indicates the bulk packing density of the Y-PSZ within the matrix, which is formed by the binder and pores, surrounding the starch particles. The addition of starch increased the amount of latex required to bind the particles, thereby increasing the F_{VL}/F_{VZ} ratio and decreasing the Y-PSZ packing density. This behavior has also been observed by our group in previous studies [13,15]. Since a low amount of starch was added to the tape the bulk packing density of the Y-PSZ powder was slightly reduced (Table 1).

The relative sintered density of the tapes prepared with and without starch was 68.6 and 87.3% of the theoretical density, respectively. The tapes prepared without starch did not achieve full densification at 1500 °C; this observation was also noted for the porous tapes prepared with starch. Fig. 1 shows the top surface matrix of *a* tape with 16.6 vol% starch sintered at 1500 °C. The micrograph

Table 1
Composition and properties of green and sintered Y-PSZ tapes prepared with and without starch.

F_{VS} (%)	VS (%)	Green density (%TD)	F_{VL}/F_{VZ}	Y-PSZ packing density	Sintered density (%TD)
0	0	87.9	1.38	34.3	87.3
19	16.6	88.4	1.61	32.8	68.6

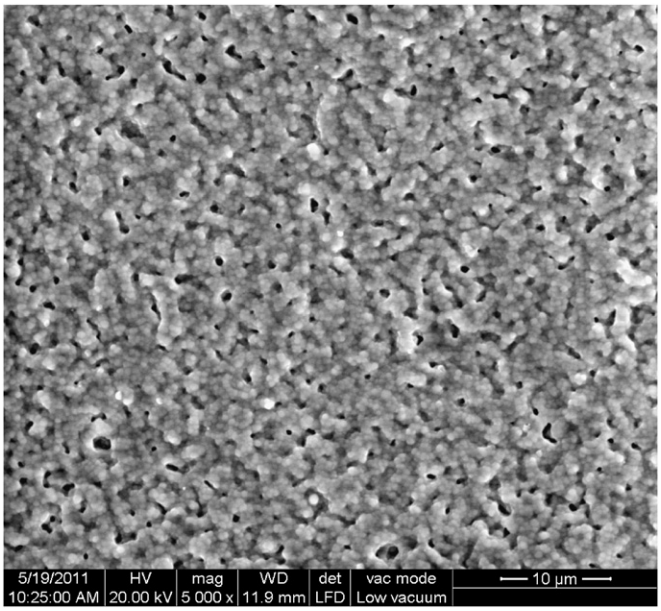

Fig. 1. SEM micrograph of the top surface matrix for a tape prepared with 16.6 vol% starch sintered at 1500 °C.

show rounded and elongated pores with length between 0.6 and 3.0 µm. The coalescence of the latex particles during drying and the pore coalescence during sintering might contribute to the enlargement of the pores in the matrix. The onset of the latex coalescence is expected to occur during the drying of the cast-tapes when the volume fraction of latex particles approaches 0.6, its maximum solids loading [20]. The latex coalescence resulted in an increase in the particle size of the latex, thereby increasing the pore size left by the latex during burnout. The pores could also coalesce during sintering so that the pore size increased. The greater the pore size, the lower the driving force for sintering and shrinkage; the enlargement of the pores leads to a decreased sintering rate [21]. Therefore, the large pores in the matrix reduced the sinterability of the Y-PSZ leading to retained closed porosity in the sintered tapes.

The total bulk porosity of the tape prepared with starch (31.4%) was higher than the volume fraction of starch in the green tape (16.6%). Since a full densification of the Y-PSZ matrix did not occur the remaining porosity did not correspond to the volume fraction of starch originally added. Therefore, the higher porosity observed with respect to the amount of added starch was due to an incomplete densification of the Y-PSZ matrix during sintering (Fig. 1).

The total bulk porosity of the tapes prepared with starch sintered at 1500 °C followed the V_S+P_0 ($F_{VL}/F_{VZ}/F_{VL0}/F_{VZ0}$) equation; where P_0 is the total porosity of the tapes without starch and the factor ($F_{VL}/F_{VZ}/F_{VL0}/F_{VZ0}$) is the F_{VL}/F_{VZ} ratio of the green tapes with starch with respect to that of the tapes without starch. The term P_0 ($F_{VL}/F_{VZ}/F_{VL0}/F_{VZ0}$) represents the additional porosity produced by the latex volume added with respect to the Y-PSZ which increased as the starch was added. Clearly, the total porosity of the tapes prepared with starch followed that predicted based on the volume fraction of starch in the green tape plus the additional porosity created by the adjustment of the formulation (high F_{VL}/F_{VZ} ratio for the tape with starch, Table 1).

Hg porosimetry was used to measure the smaller channels which corresponded to the connecting contacts voids, or necks, between much larger pores created by the original starch particles. Fig. 2 shows the differential pore size distribution curve of a sintered tape produced with 16.6 vol% starch. There was no measurable open porosity for the tapes prepared without starch; while, for the tape produced with16.6 vol% starch, channels with diameters between 0.14 and 10 µm appeared, resulting in a bimodal distribution with most frequent channel diameters of 0.6 and 2.2 µm. This open porosity (15.7%) corresponded to the connecting channels between the overlapping starch pores which resulted in a connected porous network in the sintered body. Fig. 3 shows a SEM image of a sintered tape prepared with 16.6 vol% starch. Some of the pores left by the starch interacted and an open structure interconnecting

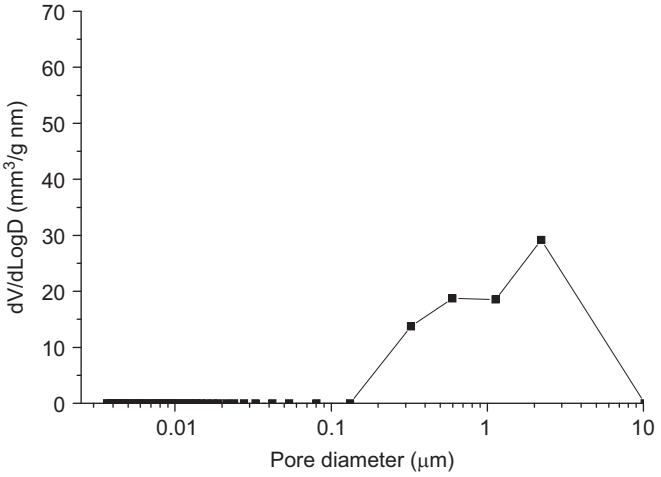

Fig. 2. Pore size distribution curve of a sintered tape developed with 16.6 vol% starch.

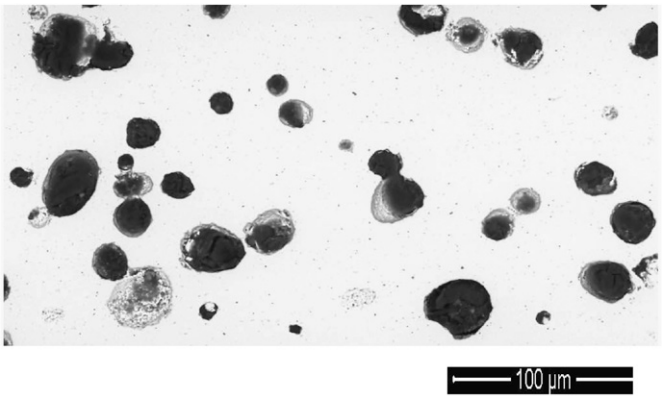

Fig. 3. SEM micrograph of a sintered tape prepared with 16.6 vol% starch.

the coarse pores was established. The interconnection open paths and channels between pores which finally result in open porosity [22].

Fig. 4 shows micrographs of the top and bottom surfaces of a sintered tape prepared with 16.6 vol% starch. The structures of the top and bottom surface matrix are shown in Fig. 4c and d. As we have mentioned the top surface was exposed to air during drying while the bottom one was in contact with the film carrier. The surfaces were different; a greater number of large pores created by the starch particles (lengths between 15 and 80 μm Fig. 4a and b) and also a greater number of smaller pores in the matrix (lengths between 0.6 and 3.0 μm) (Fig. 4c and d) were found on the top surface with respect to those on the bottom one. The starch particles migrated to the top surface during casting due to its lower density (1.45 g/cm^3) in comparison with 6.05 g/cm^3 for Y-PSZ. In addition, during drying the water flow occurred from the top surface of the tape. As was previously mentioned, the consolidation of the latex particles by coalescence is expected to occur in the later stage of the drying process as the volume fraction of latex particles approaches 0.6 [20].

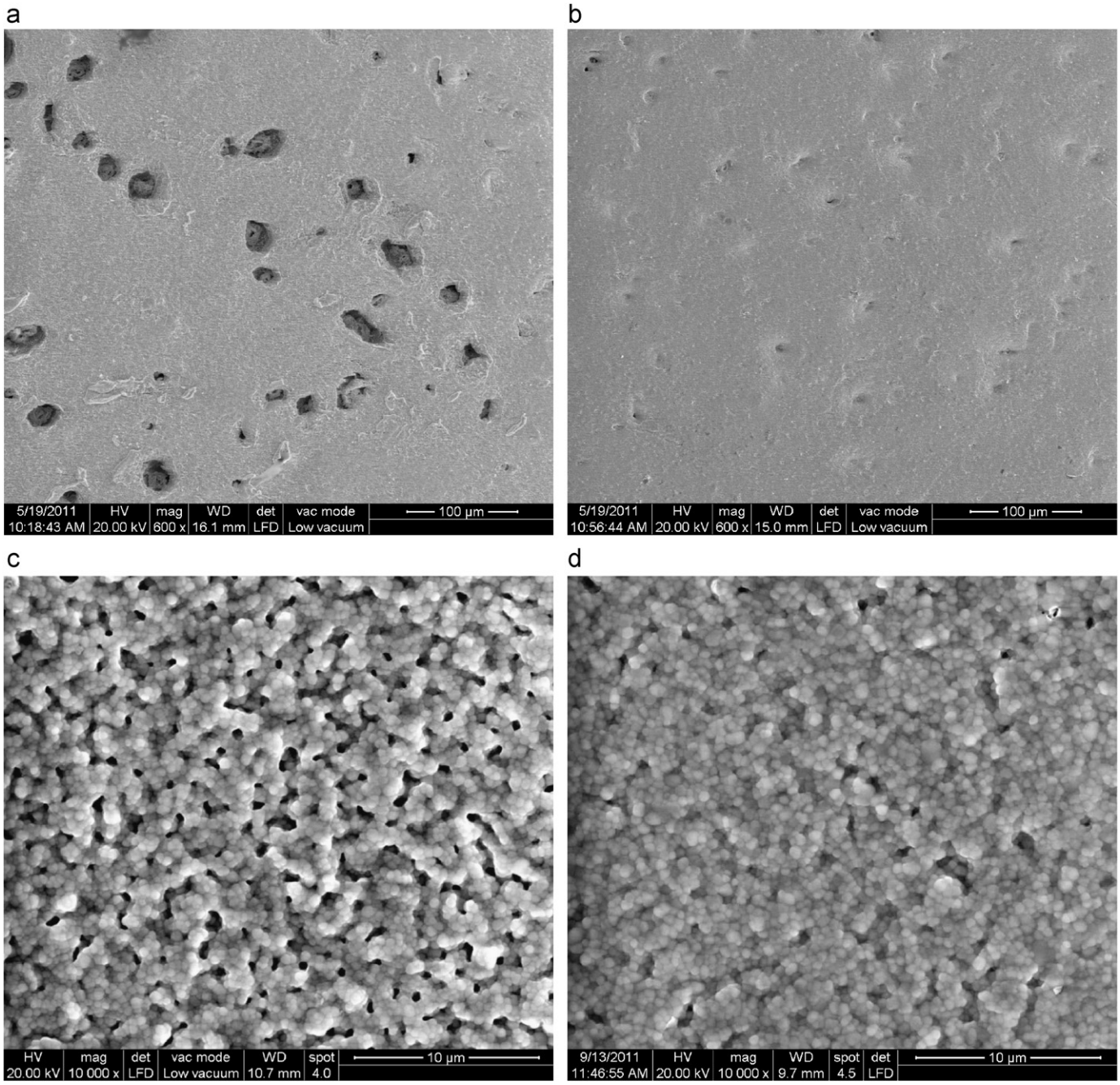

Fig. 4. SEM micrographs of the surfaces of a sintered tape developed with 16.6 vol% starch: (a) top surface; (b) bottom surface; (c) top surface matrix and (d) bottom surface matrix.

This resulted in the formation of latex particle clusters that migrated in the same direction as the solvent, to the top surface, as drying proceeded. A similar behavior was found by Martinez et al. [23] who studied the drying process of aqueous Al_2O_3-latex tape cast layers. Therefore, the top surface matrix of the cast tapes could be comprise by an assembly of latex particle clusters which increased the pore size left during burnout. These large pores reduced the Y-PSZ sintering rate within the matrix leading to retained closed porosity in the sintered tapes. The migration of the starch and the consolidated latex particles to the top surface during casting and drying, respectively, were responsible for the difference in porosity between the top and bottom surfaces of the tape, resulting in an increase in the number of pores.

Fig. 5a and b show micrographs of the top and bottom surface matrix of a sintered tape without starch. Minor porosity difference between the two surfaces could be expected since the microstructure only consisted of the small pores in the matrix. The addition of starch to the green tape markedly increased the porosity on the top surface which consisted of pores left by the starch with some connecting channels between them and the pores in the matrix. On the contrary, the porosity on the top surface of the tape without starch was composed only by a lower amount of pores in the matrix (low F_{VL}/F_{VZ} ratio for the tape without starch, Table 1 Fig. 4a–c and Fig. 5a).

The top surface of the tape prepared with starch had pores of several sizes: large pores created by the starch particles (length between 15 and 80 μm), connecting channels between the voids left by the starch (diameters between 0.14 and 10 μm) and small pores in the matrix (length between 0.6 and 3.0 μm); while the top surface of the tape prepared without starch had only the small pores in the matrix.

3.2. Fluorapatite surface coating

Two mechanisms govern the formation of a layer on a porous body during dip coating. The first mechanism is known as liquid entrainment, and occurs as the plate-like specimen is withdrawn from the slurry faster than the liquid can drain from its surface, leaving a thin slurry film [18]. This film thickness, h, is given by

$$h = 0.94(\gamma/\delta g)^{1/2} Ca^{2/3} \quad (6)$$

Ca is the capillary number given by [18]

$$Ca = \eta V/\gamma \quad (7)$$

where γ is the surface tension, δ is the slurry density, g is the gravity acceleration, η is the slurry viscosity and V is the withdrawal velocity. As the liquid from the thin layer of slurry evaporates, a thin coating of ceramic particles remains on the surface of the specimen. The second mechanism is a slip-casting phenomenon and occurs because the tapes, when dipped, are slightly porous and dry. The capillary suction caused by the porous substrate drives ceramic particles to concentrate at the substrate-suspension boundary, and a wet membrane, or cake, is formed, as in the slip casting process [19]. In this capillary filtration, the driving force is the capillary suction pressure caused by all the pores on the surface of the substrate. Fluid flow through the consolidated layer and into the porous body is governed by Darcy's law, which can be integrated and simplified (assuming that the permeability of the substrate is much larger than that of the layer) to express the thickness of the sintered layer, L, as a function of time, t, in the form [19]

$$L = 2\beta(\varepsilon_s \gamma k_m t/\eta\alpha R)^{1/2} \quad (8)$$

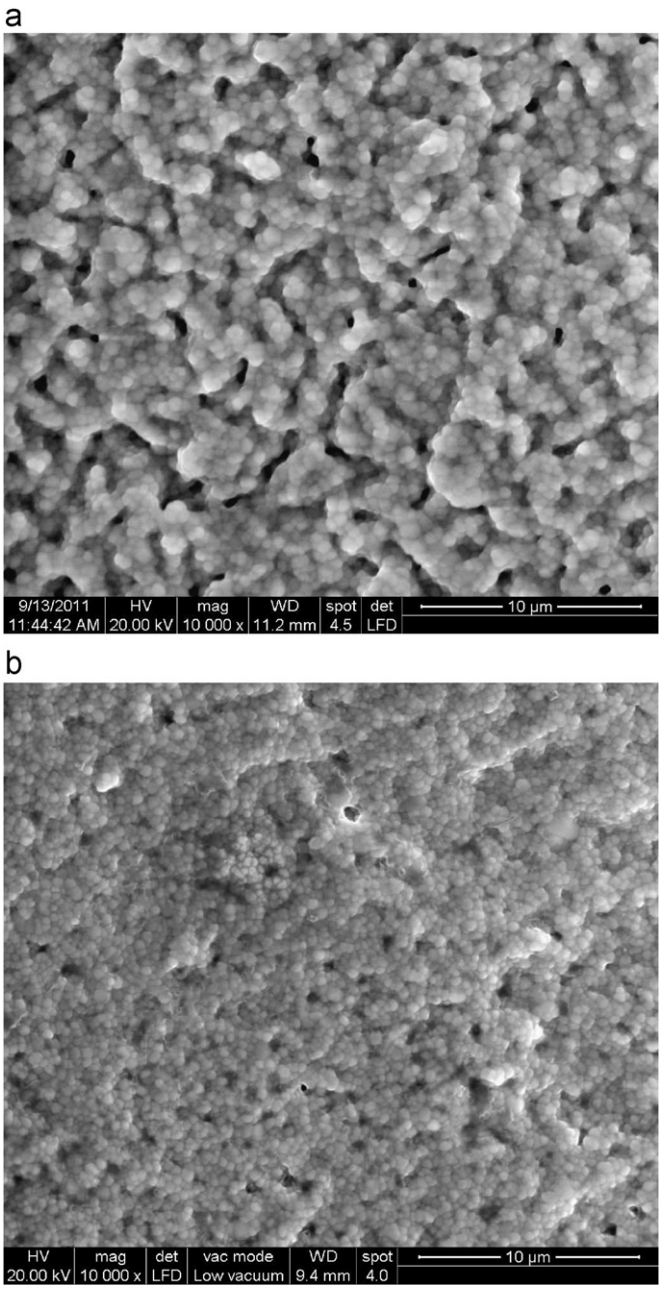

Fig. 5. SEM micrographs of the surfaces of a sintered tape prepared without starch: (a) top surface matrix and (b) bottom surface matrix.

β and α are defined as

$$\beta = \varphi_m/(1/\varepsilon_m); \quad \alpha = (\varphi_0/\varphi_m)-1 \tag{9}$$

where φ_0 and φ_m are the volume fraction of the particles in the suspension and in the wet layer, respectively, ε_m is the porosity of the sintered layer, ε_s is the porosity of the substrate, k_m is the permeability of the wet layer and R represents the pores radius.

The Eq. (8) shows that when the suspension and substrate are fixed, the layer thickness squared increases linearly with the dipping time. It also implies that the structure of the porous substrate and layer, and the properties of the suspension have close relation to the layer formation process. When the properties of the suspension (solid volume fraction, viscosity) and the structure of the layer remain constant, the porosity and pore diameter of the substrate have much influence on the layer formation.

Fig. 6a and b show the layer thickness and the layer thickness squared, respectively, versus immersion time for the top and bottom surfaces of the different tapes dip coated in the same fluorapatite suspension (27.4 vol%, η 105.9 mPa s at 542 s^{-1}). The increase in the immersion time produced significantly thicker layers up to reaching saturation of the tapes at 120 s. A linear relation between the thickness squared and the dipping time up to 120 s was found (Fig. 6b), suggesting that these data were in good agreement with the Eq. (8) for the casting mechanism.

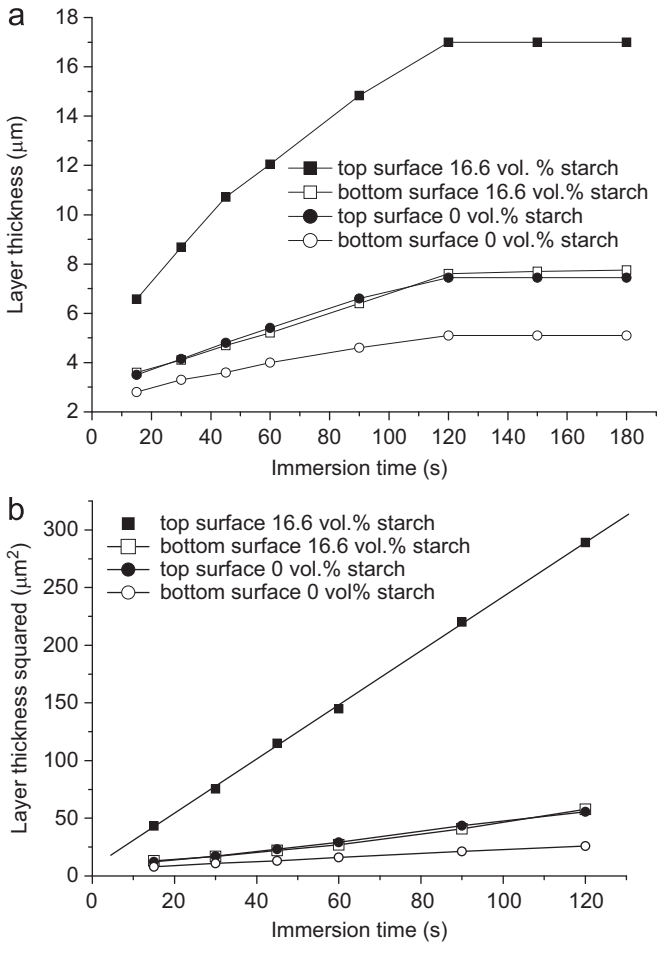

Fig. 6. Layer thickness (a) and layer thickness squared (b) versus immersion time for the top and bottom surfaces of the different tapes dip coated in the same fluorapatite suspension.

The lines in Fig. 6b did not pass through the origin instead they intersected the y-vertical axis at the same thickness value of about 2.5 μm; as we have previously mentioned the first mechanism in the layer formation was the liquid entrainment which leaved a thin slurry film on the tape surface (Eq. 6). As the data for the different substrates were obtained by using identical withdrawal velocity and suspension, the same thickness of the film adhered, h, could be expected. Thus, the film thickness given by Eq. (6) was not dependent on the structures of the porous surface. These results indicated that liquid entrainment was the dominant mechanism for layer formation at the initial stage.

A different slope of the lines for the top and bottom surfaces of the tapes prepared with and without starch was found (Fig. 6b). For each tape, the slope was higher for the top surface compared with that for the bottom one. Thus, the casting rate at the top surface of each tape was greater than that at the bottom surface. This behavior could be explained by examining the microstructure of the surfaces (Figs. 4 and 5). For the tapes prepared with starch, a greater number of large pores created by the starch particles and also a greater number of smaller pores in the matrix were found on the top surface with respect to those on the bottom one. The greater porosity and the larger number of smaller pores increased the casting rate (Eq. 8) of the top surface producing thicker dip-coated layers.

The absence of starch in the green tape reduced the porosity difference between the two surfaces (Fig. 5a and b) since the tape had only a lower amount of the small pores in the matrix, which were principally located on the top surface. As a consequence, minor difference in the casting rate between the two surfaces was observed for the tapes produced without starch. Layers formed on the top surface were found to be about 55 and 32% thicker than those formed on the bottom surface, for the tapes developed with 16.6 and 0 vol% starch, respectively.

Fig. 7 shows a micrograph of a sintered tape prepared with starch coated with fluorapatite. It showed the thinner dip-coated layer formed on the bottom surface relative to that on the top one. The highest casting rate at the top surface of the tape prepared with starch produced the thickest layer of about 17 μm.

The cross-sectional morphology of the FA layer on porous zirconia and the microstructure of the FA coating layer are shown in Fig. 8a and b, respectively. The FA layer uniformly covered the surface of the substrate.

Fig. 9 shows the weight gain of sintered tapes prepared with and without starch as a function of the immersion time. The weight gain increased linearly with the immersion time up to reaching saturation of the tapes at 120 s. The weight gain reached at 120 s was about twice higher for the tape produced with 16.6 vol% starch. This was in

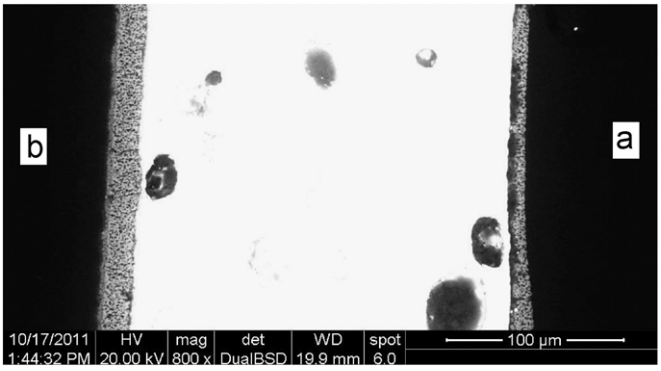

Fig. 7. SEM micrograph of a sintered tape prepared with starch coated with fluorapatite (immersion time = 180 s): (a) bottom surface and (b) top surface.

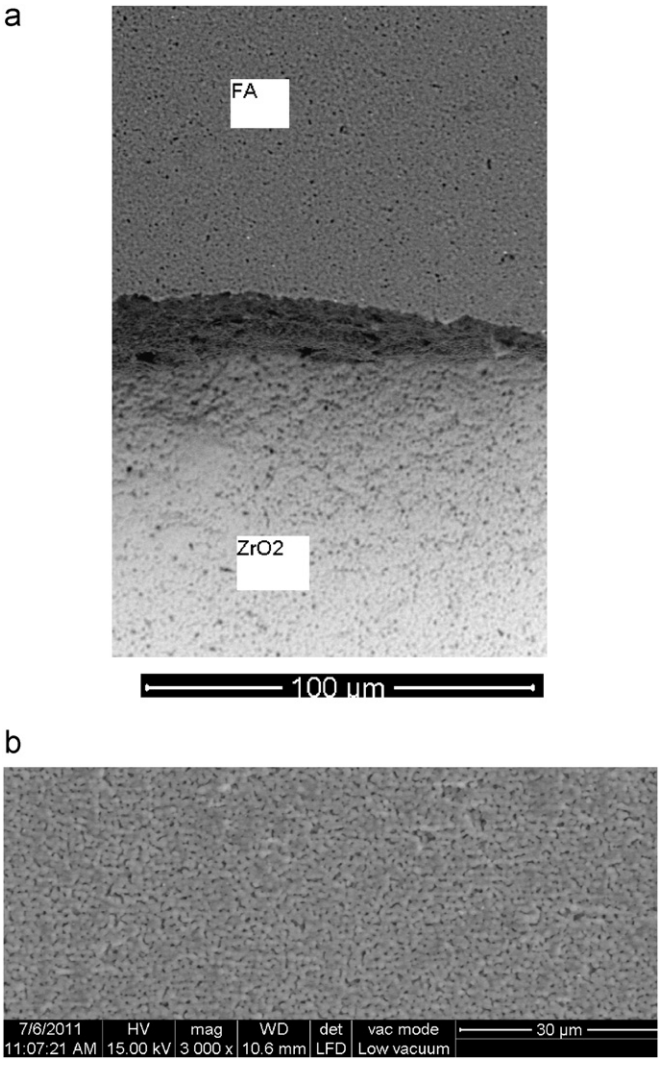

Fig. 8. (a) Cross-sectional morphology of the FA layer on porous zirconia and (b) Microstructure of the FA coating layer.

accordance with the layer thickness results; thus, the sum up of the layer thickness on both surfaces for the tape prepared with starch was approximately twice higher than that for the tape developed without starch (Fig. 6a). As the

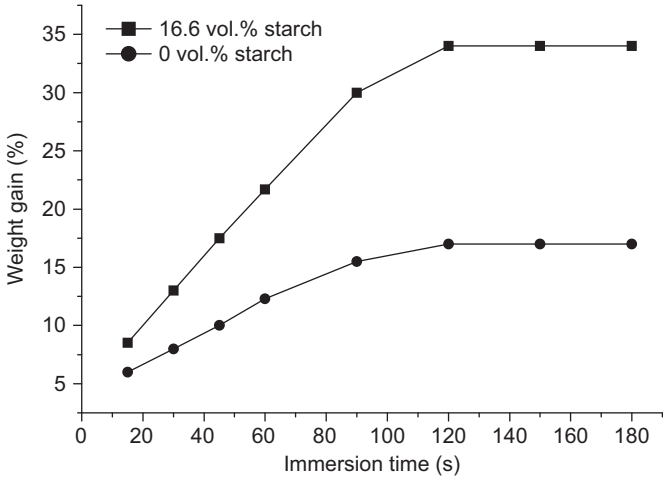

Fig. 9. Weight gain of sintered tapes prepared with and without starch as a function of the immersion time.

tapes prepared with and without starch had the same dimensions, similar sintering shrinkage and density of the FA layer, a proportionally between the weight gain and the layer thickness could be expected. The greater slope of the weight gain versus t line for the tape produced with starch was consistent with the greater slope of the L^2 versus t lines (Fig. 6b and Fig. 9). The top surface of this tape mainly contributed to increase the thickness and consequently the weight gain.

4. Conclusions

Thin fluorapatite layers on porous Y-PSZ substrates have been fabricated by dipping porous zirconia tapes into aqueous 27.4 vol% fluorapatite slurries. Porous Y-PSZ tapes with volume fraction of porosity of 31.4% were developed using starch and an acrylic latex as fugitive additive and binder, respectively. For comparison, Y-PSZ tapes with 12.7 vol% porosity were fabricated without starch.

The formation of a thin layer on the surface of the tapes was governed by liquid entrainment at the initial stage and slip casting for longer immersion times. Since the withdrawal velocity and suspension properties were fixed the same initial thickness of the layer adhered was found for the different substrates. For immersion times > 0, the data for FA layer formation were in good agreement with the slip casting model.

The casting rate was observed to be strongly influenced by the structure of the tape surfaces. The casting rate at the top surface of both tapes was greater than that at the bottom surface. This difference was attributed to the greater porosity of the top surface with respect to that of the bottom one and was more pronounced for the tape prepared with starch. For these tapes, the migration of the starch and the consolidated latex particles to the top surface during tape casting and drying, respectively, resulted in an increase in porosity of the top surface after

sintering relative to that of the bottom surface. While for the tapes developed without starch, only a lower amount of consolidate latex particles migrated to the top surface during drying. Thus, minor difference in porosity and consequently in the casting rate between the top and bottom surfaces was observed. Layers formed on the top surface were found to be about 55 and 32% thicker than those formed on the bottom surface, for the tapes prepared with 16.6 and 0 vol% starch, respectively. For the tapes developed with starch, the greater porosity and also the greater number of smaller pores in the matrix of the top surface produced the thickest dip coated layers of about 17 μm.

References

[1] S. Weiner, H.D. Wagner, The material bone: structure-mechanical function relations, Annual Review of Materials Science 28 (1998) 271–298.

[2] M. Vallet-Regí, J.M. González-Calbet, Calcium phosphates as substitution of bone tissues, Progress in Solid State Chemistry 32 (2004) 1–31.

[3] S.V. Dorozhkin, Nanodimensional and nanocrystalline apatites and other calcium orthophosphates in biomedical engineering, biology and medicine, Materials 2 (2009) 1975–2045.

[4] W. Suchanek, M. Yoshimura, Processing and properties of hydroxyapatite-based biomaterials for use as hard tissue replacement, Journal of Materials Research 13 (1998) 94–117.

[5] L.L. Hench, Bioceramics: from concept to clinic, Journal of the American Ceramic Society 74 (7) (1991) 1487–1510.

[6] H.W. Kim, S.Y. Lee, C.J. Bae, Y.J. Noh, H.E. Kim, H.M. Kim, J.S. Ko, Porous ZrO_2 bone scaffold coated with hydroxyapatite with fluorapatite intermediate layer, Biomaterials 24 (2003) 3277–3284.

[7] H.W. Kim, B.H. Yoon, Y.H. Koh, H.E. Kim, Processing and performance of hydroxyapatite/fluorapatite double layer coating on zirconia by the powder slurry method, Journal of the American Ceramic Society 89 (8) (2006) 2466–2472.

[8] K. de Groot, R.G.T. Geesink, C.P.A.T. Klein, P. Serekian, Plasma-spayed coatings of hydroxyapatite, Journal of Biomedical Materials Research 21 (1987) 1375–1381.

[9] D.M. Liu, H.M. Chou, J.D. Wu, plasma-sprayed hydroxyapatite coatings: effect of different calcium phosphate ceramics, Journal of Materials Science: Materials in Medicine 5 (1994) 147–153.

[10] W. Weng, J.L. Baptista, Sol–gel derived porous hydroxyapatite coatings, Journal of Materials Science: Materials in Medicine 9 (1998) 159–163.

[11] T. Brendel, A. Engel, C. Russel, Hydroxyapatite coatings by a polymeric route, Journal of Materials Science: Materials in Medicine 3 (1992) 175–179.

[12] M.P. Albano, L. Genova, L.B. Garrido, K. Plucknett, Processing of porous yttria-stabilized zirconia by tape-casting, Ceramics International 34 (2008) 1983–1988.

[13] M.P. Albano, L.B. Garrido, K. Plucknett, L. Genova, Processing of porous yttria-stabilized zirconia tapes: Influence of starch content and sintering temperature, Ceramics International 35 (5) (2009) 1783–1791.

[14] M.P. Albano, L.B. Garrido, K. Plucknett, L. Genova, Effect of starch filler content and sintering temperatura on the processing of porous 3Y-ZrO2 ceramics, Journal of Materials Processing Technology 209 (1) (2009) 590–598.

[15] M.P. Albano, L.B. Garrido, K. Plucknett, L. Genova, Influence of starch content and sintering temperature on the microstructure of porous yttria-stabilized zirconia tapes, Journal of Materials Science 44 (10) (2009) 2581–2589.

[16] M.P. Albano, L.B. Garrido, Rheological properties of concentrated aqueous fluorapatite suspensions, Ceramics International 36 (2010) 1779–1786.

[17] M.P. Albano, L.B. Garrido, Processing of concentrated aqueous fluorapatite suspensions by slip casting, Journal of Materials Science 46 (15) (2011) 5117–5128.

[18] M.G. Pontin, F.F. Lange, A.J. Sánchez-Herencia, R. Moreno, Effect of unfired tape porosity on surface film formation by dip coating, Journal of the American Ceramic Society 88 (10) (2005) 2945–2948.

[19] Y. Gu, G. Meng, A model for ceramic membrane formation by dip-coating, Journal of the European Ceramic Society 19 (1999) 1961–1966.

[20] J.E. Smay, J.A. Lewis, Structural and property evolution of aqueous-based lead zirconate titanate tape-cast layers, Journal of the American Ceramic Society 84 (11) (2001) 2495–2500.

[21] D. Kolar, On the role of sintering research in ceramic engineering in sintering processes, Materials Science Research 13 (1979) 335–367.

[22] S.F. Corbin, P.S. Apté, Engineered porosity via tape casting, lamination and the percolation of pyrolyzable particulates, Journal of the American Ceramic Society 82 (7) (1999) 1693–1701.

[23] C.J. Martinez, J.A. Lewis, Rheological, structural and stress evolution of aqueous Al_2O_3–latex tape-cast layers, Journal of the American Ceramic Society 85 (10) (2002) 2409–2416.